

Antihydrogen Synthesis in a Double-Cusp Trap

Naofumi KURODA¹, Minori TAJIMA^{1,2}, Balint RADICS², Pierre DUPRÉ², Yugo NAGATA³,
Chikato KAGA⁴, Yasuyuki KANAI², Marco LEALI^{5,6}, Evandro LODI RIZZINI^{5,6}, Valerio
MASCAGNA^{5,6}, Takuya MATSUDATE¹, Horst BREUKER⁷, Hiroyuki HIGAKI⁴, Yasuyuki MATSUDA¹,
Stefan ULMER⁸, Luca VENTURELLI^{5,6}, and Yasunori YAMAZAKI²

¹*Institute of Physics, Graduate School of Arts and Sciences, University of Tokyo, 3-8-1 Komaba,
Meguro-ku, Tokyo 153-8901, Japan*

²*Atomic Physics Research Unit, RIKEN, 2-1 Hirosawa, Wako-shi, Saitama 351-0198, Japan*

³*Department of Applied Physics, Tokyo University of Agriculture and Technology, 2-24-16
Nakacho, Koganei-shi, Tokyo 184-8588, Japan*

⁴*Graduate School of Advanced Sciences of Matter, Hiroshima University, 1-3-1 Kagamiyama,
Higashi-Hiroshima, Hiroshima 739-8530, Japan*

⁵*Dipartimento di Ingegneria dell'Informazione, Università di Brescia, Brescia 25133, Italy*

⁶*INFN, Gruppo Collegato di Brescia, Brescia 25133, Italy*

⁷*CERN, Genève 1211, Switzerland*

⁸*Ulmer Initiative Research Unit, RIKEN, 2-1 Hirosawa, Wako-shi, Saitama 351-0198, Japan*

E-mail: kuroda@phys.c.u-tokyo.ac.jp

(Received June 14, 2016)

The ASACUSA CUSP experiment plans a high precision spectroscopy of the ground-state hyperfine splitting of antihydrogen to test CPT symmetry. To perform this, a Rabi-like antiatomic beam method has been developed with a novel double-cusp trap. Antihydrogen atoms were synthesized in the double-cusp trap by directly injecting antiprotons from an accumulation trap into a positron plasma. By adjusting the energy difference between the incoming antiproton beam and the positron plasma, a high-rate production of antihydrogen atoms was observed.

KEYWORDS: antihydrogen synthesis, double-cusp trap

1. Introduction

CPT symmetry is one of the most important symmetries of the Standard Model of particle physics. In order to test CPT symmetry experimentally, the ASACUSA collaboration has developed a Rabi-like antiatomic beam technique to measure hyperfine splitting of the ground-state antihydrogen ($\bar{\text{H}}$) atom [1, 2]. The key of the antiatomic beam experiment is to synthesize a large number of $\bar{\text{H}}$ atoms at several meV energy in a cusp magnetic field whose field gradient focuses $\bar{\text{H}}$ atoms [3].

2. Apparatus

Figure 1 shows the experimental setup. Constituents of $\bar{\text{H}}$ are antiproton (\bar{p}) and positron (e^+). Energetic \bar{p} s and e^+ s are stored in electromagnetic traps and cooled at the chemical energy scale, eV or less, for an efficient synthesis of antihydrogen atoms.

One of the trap is an antiproton accumulator, the MUSASHI trap, which consists of a superconducting solenoid and a stack of multiple-ring electrodes [4]. Millions of \bar{p} s are typically accumulated in the MUSASHI trap.

Positrons are provided by a ^{22}Na radioactive source. A solid Ne moderator is used to moderate e^+ s. By interaction with N_2 gas, the e^+ are accumulated in the second electromagnetic trap which is

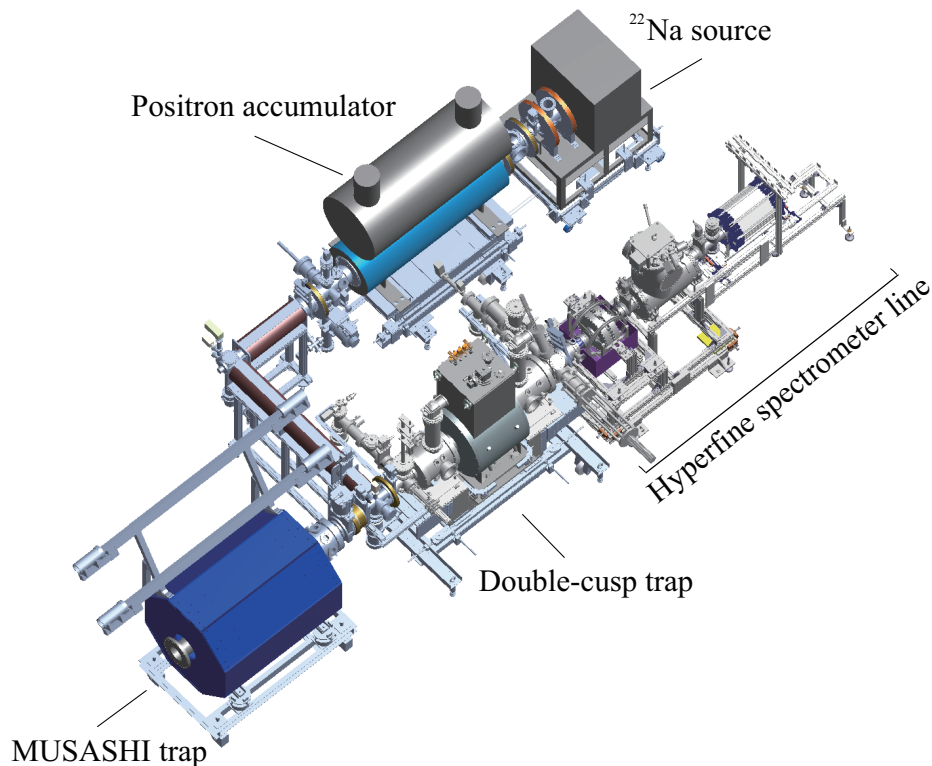


Fig. 1. A 3D-schematic view of the cusp experiment.

the positron accumulator shown in Fig 1.

Antiprotons and positrons are mixed in the third electromagnetic trap with a cusp magnetic field by an anti-Helmholtz coil assembly. Antihydrogen atoms are synthesized in this trap. The field gradient of the cusp magnetic field exerts a force on \bar{H} atoms. Anti-atoms in low-field-seeking states are preferentially focused, while high-field-seekers are diverged. This feature of the cusp magnetic field results in a spin-polarized beam [3, 5].

By using a single-cusp configuration with a combination of a superconducting anti-Helmholtz coil and a stack of multiple-ring electrodes (MRE), antihydrogen synthesis [6] and extraction of an antihydrogen beam [2] were successfully demonstrated.

In order to increase the intensity and to improve the polarization of the \bar{H} beam, a double-cusp trap was developed. The double-cusp trap is composed of two sets of anti-Helmholtz coils aligned along the axis and the MRE. Figure 2 (a) shows the field strength on the axis of the double-cusp magnet. As was discussed in Ref. [7], the configuration of the double-cusp magnetic field improves the focusing performance by a factor of 10 .

The MRE as shown in Fig. 2 (b) is located inside the double-cusp magnet. By applying different voltages on each electrode of the MRE, a nested-well configuration is prepared as shown in Fig. 2 (c). Electrical connections to the MRE are filtered to suppress external noises which affect the temperature of confined plasmas.

A positron plasma which typically contained $(3-7) \times 10^7$ particles was confined in the well at $z \sim -0.27$ m in Fig. 2. About 3×10^5 of slow \bar{p} s were captured at the mixing region and mixed with e^+ s. A field ionization well (FIW) at $z = -0.06$ to 0.03 m shown as shaded area in Fig. 2 (c) was prepared at the downstream of the mixing region, where a strong electric field was provided to field-ionize antihydrogen atoms at a high-Rydberg state [6, 8]. The maximum field strength on the

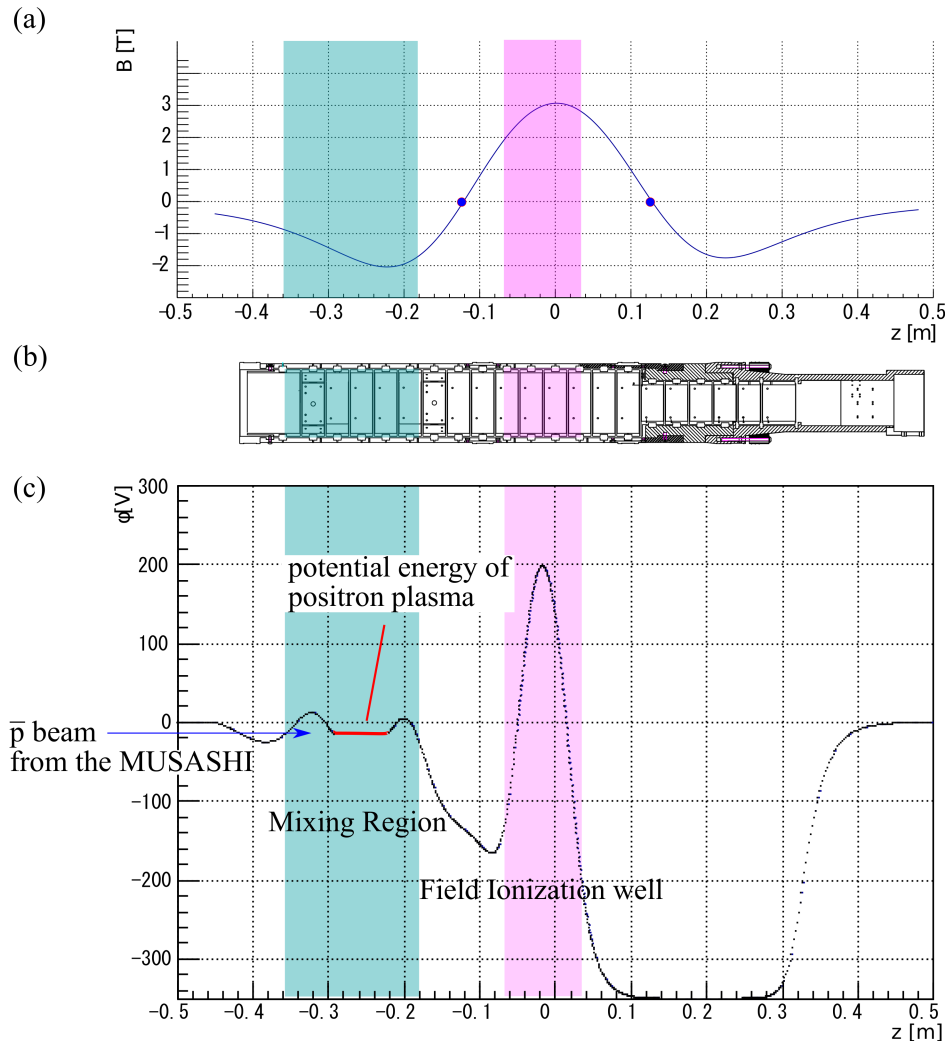


Fig. 2. (a) The magnetic field strength along the axis the beam axis. (b) A cross sectional view of the CUSP MRE. (c) The nested-well configuration for synthesis of \bar{H} .

axis was around 103 V/cm, which ionized antihydrogens at $n > 42$. Antiprotons accumulated in the FIW were released for annihilation. The annihilation products, mainly charged pions, were detected by a pion tracking detector.

3. Experiment

Figure 3 (a) shows the number of \bar{p} s originated from field-ionized \bar{H} atoms as a function of time since the start of the mixing when the 150 eV \bar{p} beam was injected into $3 \times 10^7 e^+$ s. The FIW was repeatedly opened for 100 ms every 5 s during the measurement. The yield of field-ionized \bar{H} increased in the first 20 s and then decreased in the next 20 s. This behavior implies that the positron plasma was initially heated up by the incoming \bar{p} beam with the wider energy spread, ca. 20 eV.

A plasma at lower temperature gives higher yield of \bar{H} [9]. It is necessary to mix \bar{p} s with a e^+ plasma by keeping their relative energy difference as small as possible in order to avoid heating up the plasma. The potential energy of the positron plasma was adjusted at the same energy of the incoming beam. In addition, the energy width of the incoming \bar{p} beam was improved by a more

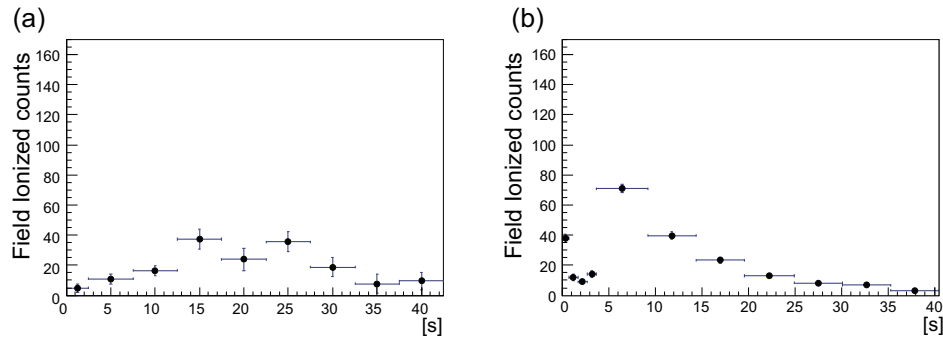


Fig. 3. (a) The number of field-ionized $\bar{\text{H}}$ monitored by opening FIW every 5 s after the 150 eV beam was injected (b) With 20 eV. During the first 3s, FIW was dumped every 0.75 s then the interval was 5 s.

adiabatic transport from the MUSASHI to the double-cusp trap as was discussed in Ref. [10]. The result shown in Fig. 3 (b) was obtained when the 20 eV $\bar{\text{p}}$ beam was injected into the e^+ plasma whose potential energy was adjusted within an error of 2 eV. A prompt peak within 0.75 s after the start of the mixing was followed by the second broad peak within 10 s. The first component was due to $\bar{\text{p}}\text{s}$ with a close energy against the potential of the e^+ plasma. The second peak was assumed to be related to $\bar{\text{p}}\text{s}$ with a higher energy, which heated up the plasma as in the case of 150 eV non-adiabatic beam transportation.

During the mixing, the annihilation positions of $\bar{\text{p}}\text{s}$ and $\bar{\text{H}}$ atoms were monitored by the pion tracking detector. For the case of the 20 eV- $\bar{\text{p}}$ beam, Fig. 4 shows time slices of antiproton annihilation distribution along the trap axis for six time ranges as indicated on the top of each panel. For the first 1 s, a single peak can be recognized around the position corresponding to the center of the e^+ plasma. Then the peak becomes broader. After 5–10 s, the peak starts to split into two, which indicates the axial separation of $\bar{\text{p}}\text{s}$ towards the two potential maxima [2, 6].

The synthesis of $\bar{\text{H}}$ does not depend only on the temperature but also on the density of the e^+ plasma [9]. Figure 5 (a) is the case when a smaller number of e^+ , 4×10^7 , i.e., lower density, were prepared. The average number of field-ionized $\bar{\text{H}}$ was around 250, while ca. 40 events were detected in the first 0.75 s. The case of a larger number, 7×10^7 , i.e., higher density, is shown in Fig. 5 (b), which indicates a higher rate of $\bar{\text{H}}$ production at the first 0.75 s. Here the offset of the nested-well was adjusted for the different space charge of plasmas. About 140 $\bar{\text{H}}$ atoms were field-ionized within the first 0.75 s, i.e., 3 times more as compared with 4×10^7 e^+ case described above. The total number of count of field-ionized $\bar{\text{H}}$ was 390. By assuming isotropic angular distribution of $\bar{\text{H}}$ atoms, the formation efficiency from antiprotons to $\bar{\text{H}}$ atoms in Rydberg states was 16% from the solid angle of the FIW against the nested-well, while in the case of 150 eV injection it was only around 6%.

4. Summary

The double-cusp trap was developed. Antihydrogen synthesis in the double-cusp trap was confirmed. Though there still remains a room to improve the energy width of the incoming beam, a factor of 2.7 more efficient production of $\bar{\text{H}}$ was achieved by using the 20 eV $\bar{\text{p}}$ beam, by adjusting the floating voltage of the nested-well and the number of e^+ s. The plasma conditions such as its temperature and density is also needed to be investigated further, since the collisional deexcitation of Rydberg $\bar{\text{H}}$ is also expected to be important to obtain ground-state $\bar{\text{H}}$ atoms [11].

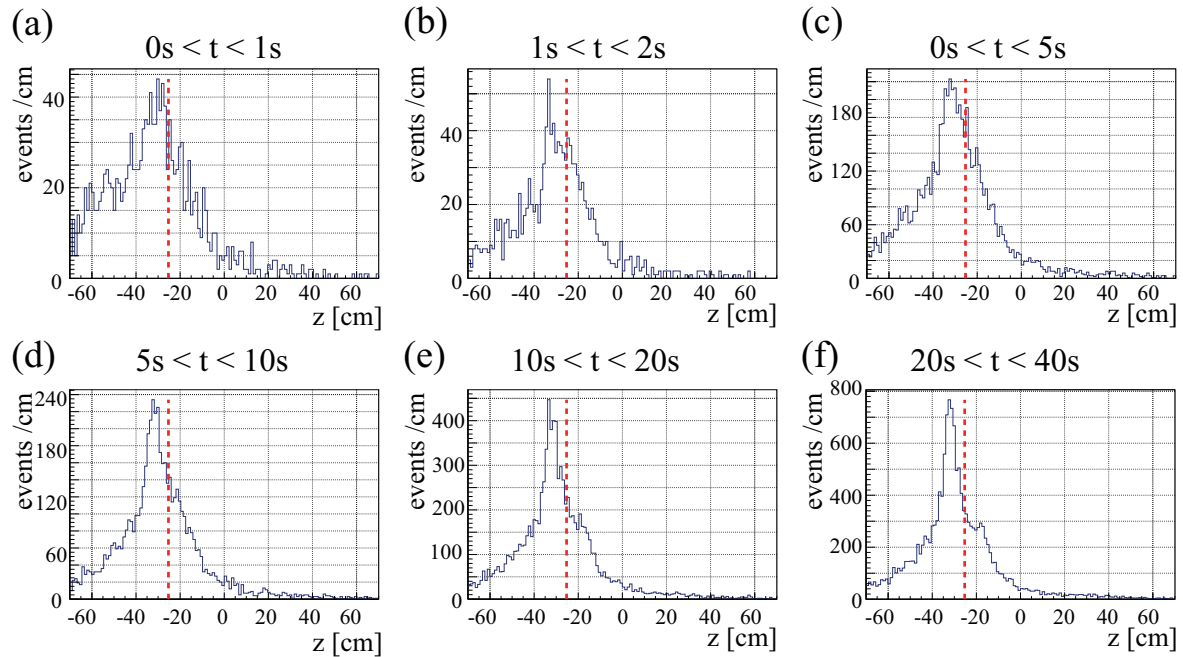


Fig. 4. Time slices of annihilation position distribution along the trap axis. The red dotted line corresponds to the center of the e^+ plasma. Antiprotons were injected at $t=0$ s.

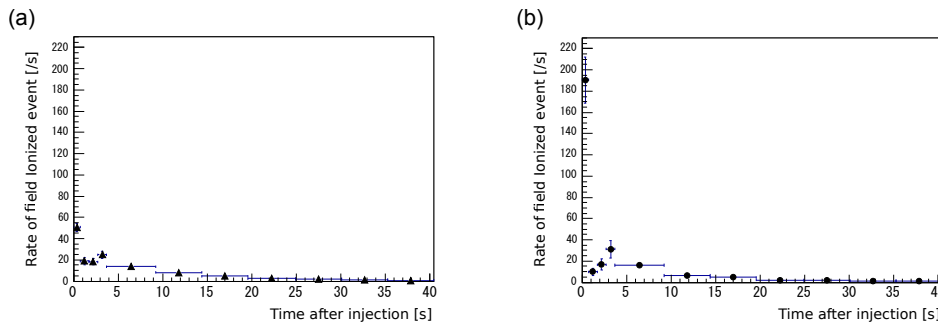


Fig. 5. The rate of field-ionization of \bar{H} for different e^+ numbers with the same radial distribution. (a) $N = 4 \times 10^7$, (b) $N = 7 \times 10^7$.

Acknowledgments

This work was supported by the Grant-in-Aid for Specially Promoted Research (19002004 and 24000008) of Japanese Ministry of Education, Culture, Sports, Science and Technology (MEXT), Special Research Projects for Basic Science of RIKEN, RIKEN IRU program, Università di Brescia, and Istituto Nazionale di Fisica Nucleare.

References

- [1] E. Widmann, M. Diermaier, B. Juhász, C. Malbrunot, O. Massiczek, C. Sauerzopf, K. Suzuki, B. Wünschek, J. Zmeskal, S. Federmann, N. Kuroda, S. Ulmer, and Y. Yamazaki: *Hyperfine Interactions* **215** (2013) 1.
- [2] N. Kuroda, S. Ulmer, D. J. Murtagh, S. Van Gorp, Y. Nagata, M. Diermaier, S. Federmann, M. Leali, C. Malbrunot, V. Mascagna, O. Massiczek, K. Michishio, T. Mizutani, A. Mohri, H. Nagahama, M. Oht-

- suka, B. Radics, S. Sakurai, C. Sauerzopf, K. Suzuki, M. Tajima, H. A. Torii, L. Venturelli, B. Wünschek, J. Zmeskal, N. Zurlo, H. Higaki, Y. Kanai, E. Lodi Rizzini, Y. Nagashima, Y. Matsuda, E. Widmann, and Y. Yamazaki: *Nat. Commun.* **5** (2014) 3089.
- [3] A. Mohri and Y. Yamazaki: *Europhys. Lett.* **63** (2003) 207.
- [4] N. Kuroda, H. A. Torii, Y. Nagata, M. Shibata, Y. Enomoto, H. Imao, Y. Kanai, M. Hori, H. Saitoh, H. Higaki, A. Mohri, K. Fujii, C. H. Kim, Y. Matsuda, K. Michishio, Y. Nagashima, M. Ohtsuka, K. Tanaka, and Y. Yamazaki: *Phys. Rev. ST Accel. Beams* **15** (2012) 024702.
- [5] Y. Nagata and Y. Yamazaki: *New J. Phys.* **16** (2014) 083026.
- [6] Y. Enomoto, N. Kuroda, K. Michishio, C. H. Kim, H. Higaki, Y. Nagata, Y. Kanai, H. A. Torii, M. Corradini, M. Leali, E. Lodi-Rizzini, V. Mascagna, L. Venturelli, N. Zurlo, K. Fujii, M. Ohtsuka, K. Tanaka, H. Imao, Y. Nagashima, Y. Matsuda, B. Juhász, A. Mohri, and Y. Yamazaki: *Phys. Rev. Lett.* **105** (2010) 243401.
- [7] Y. Nagata, N. Kuroda, P. Dupré, B. Radics, M. Tajima, A. Capon, M. Diermaier, C. Kaga, B. Koblinger, M. Leali, E. Lodi Rizzini, C. Malbrunot, V. Mascagna, O. Massiczek, T. Matsudate, C. Sauerzopf, M.C. Simon, K. Suzuki, J. Zmeskal, H. Breuker, H. Higaki, Y. Kanai, Y. Matsuda, S. Ulmer, L. Venturelli, E. Widmann, and Y. Yamazaki: *in this proceedings*
- [8] G. Gabrielse, N.S. Bowden, P. Oxley, A. Speck, C.H. Storry, J.N. Tan, M. Wessels, D. Grzonka, W. Oelert, G. Schepers, T. Seifick, J. Waltz, H. Pittner, T.W. Hänsch, and E.A. Hessels (ATRAP Collaboration): *Phys. Rev. Lett.* **89** (2002) 213401.
- [9] B. Radics, D. J. Murtagh, Y. Yamazaki, and F. Robicheaux: *Phys. Rev. A* **90** (2014) 032704.
- [10] M. Tajima, N. Kuroda, P. Dupré, M. Leali, Y. Nagata, T. Matsudate, V. Mascagna, B. Radics, L. Venturelli, H. Breuker, H. Higaki, Y. Kanai, E. Lodi Rizzini, Y. Matsuda, S. Ulmer, and Y. Yamazaki: *in this proceedings*
- [11] B. Radics and Y. Yamazaki. *J. Phys. B* **49** (2016) 064007.